Single-shot Femtosecond X-Ray Holography Using Extended References

D. Gauthier,[1] M. Guizar-Sicairos,[2] X. Ge,[1] W. Boutu,[1] B. Carré,[1] J. R. Fienup,[2] and H. Merdji[1,3,*]

[1]*CEA-Saclay, IRAMIS, Service des Photons, Atomes et Molécules, 91191 Gif-sur-Yvette, France*
[2]*The Institute of Optics, University of Rochester, Rochester, New York, 14627, USA*
[3]*PULSE Institut for Ultrafast Energy Science, Stanford Linear Accelerator Center, Stanford University, 2575 Sand Hill Road, Menlo Park, California 94025, USA*

(Received 4 February 2010; revised manuscript received 15 July 2010; published 24 August 2010)

In the context of x-ray lensless imaging, we present a recent approach for Fourier transform holography based on the use of extended references. Major advances shown here rely on a high signal efficiency and on the direct image reconstruction of the object performed by a simple linear derivative. Moreover, the extended holographic reference is easy to manufacture and can be applied to a variety of imaging experiments. Here we demonstrate single-shot imaging with a table-top, laser-based coherent soft x-ray source. A spatial resolution of 110 nm was obtained with an integration time of 20 fs.

DOI: 10.1103/PhysRevLett.105.093901 PACS numbers: 42.40.−i, 42.30.Wb, 87.59.−e

Lensless imaging using coherent x rays has demonstrated great potential in recent years especially with new ultrafast coherent x-ray sources, the free electron laser (FEL) [1–4], and high harmonics generation (HHG) [5–7]. This technique has attracted much attention due to its application in ultrafast nanoscale imaging. Indeed, these bright flashes of x-ray light can capture snapshots of dynamical processes even in dense matter and at a mesoscopic scale [4]. In this context, various lensless coherent imaging schemes have been explored using x rays, including, for example, coherent diffractive imaging [8], keyhole diffractive imaging [9], and Fourier transform holography [10–12].

Imaging without image forming optics is based on the measurement of the intensity diffracted from an object illuminated by a coherent x-ray beam. In this technique the two-dimensional complex-valued object transmissivity can be retrieved from the measured far-field scattered amplitude using either iterative phase retrieval or direct holographic techniques. For Fourier transform holography (FTH) a point source in the vicinity of the object generates a reference wave that interferes with the object's scattered wave at the detector plane [10–13]. Thus, the phase and amplitude information of the object are encoded in the intensity of the holographic diffraction pattern, the hologram.

One advantage of FTH is that the complex-valued image is retrieved in a noniterative and unambiguous fashion with a simple reconstruction algorithm, namely, an inverse Fourier transform of the hologram. This is a valuable alternative to computationally intensive iterative algorithms which attempt to solve the phase retrieval problem of reconstructing an image from coherent diffractive imaging (CDI) data [8,14]. The possibility of reliably retrieving a closed-form, unique solution makes holography an attractive lensless configuration and holds potential in the recent context of ultrafast single-shot imaging using an x-ray free electron laser or a table-top high harmonic source.

In the x-ray regime, various schemes have been proposed to go beyond the limitations imposed in standard holography, as, for example, the use of complicated references [15], large references [16], or multiples references [17]. More recently a holographic scheme based on a uniformly redundant array of references was successfully demonstrated at the Hamburg FLASH soft x-ray free electron laser [18]. Although this scheme increases the signal to noise ratio (SNR) of the reconstruction, the direct inversion of the hologram relies on quantitative knowledge of this reference structure. The latter is significantly affected by the difficult manufacturing process. Such an approach is also difficult to scale down to fine resolution accessible at hard x-ray wavelengths where a reference and a reconstruction procedure robust to manufacturing errors should be used.

In standard FTH there is a compromise in the determination of the size of the reference point source between the two requirements: (i) the resolution given by the reference size, and, (ii) the flux through the reference for observing interference fringes with a good contrast [15,16]. The hologram fringe visibility depends on the relative amplitudes of the fields diffracted by the object and the reference, respectively, and is clearly maximum when these amplitudes are equal. The use of extended references allows increasing the fringe visibility, especially at larger scattering angles (which correspond to higher resolution) where the scattering signal may be weak. The hologram is subsequently more efficiently recorded than in standard FTH. This improves the image reconstruction with substantially enhanced quality and resolution as compared with a point source reference.

In this Letter we demonstrate single-shot femtosecond x-ray holography using a recently developed approach; holography with extended reference by autocorrelation

linear differential operation (HERALDO) [19–21]. This lensless imaging scheme preserves the deterministic reconstruction properties of FTH. The analytical uniqueness of the solution directly retrieved as a complex-valued image from the hologram. HERALDO is a more general approach to FTH, using boundary waves of more general extended objects as holographic references. The reconstruction procedure is robust and simple to implement. It is based on the application of linear differential operators to the field autocorrelation, i.e., the inverse Fourier transform of the hologram. In our setup, the extended references used around the nanoscale test object "φ" are linear slits [see Fig. 1]. The directional derivative (in the direction of the slit) is applied during the reconstruction process, which then provides two independent reconstructions of the object "φ", each associated with the slit extremities [Figs. 1 and 2]. As in FTH, each reconstruction has an associated twin image that does not provide additional information. The HERALDO image processing is indicated by the $\frac{d}{d\rightarrow}F^{-1}\{\text{hologram}\}$ symbol in Fig. 1.

The test object and the linear reference slits were patterned using a focused ion beam at a resolution of about 20 nanometers on a freestanding Si_3N_4 membrane of 225 nm thickness. A 50 nm layer of gold was deposited on the membrane so that the sample has a pure amplitude transmittance. The test object "φ" has a 2 μm $\times$ 1.7 μm overall size, with 200 nm to sub-100 nm details [Fig. 2(a)]. The horizontal and vertical reference slits have a width of, respectively, 130 and 145 nm. The two slits are slightly longer than the object dimensions, and they are etched at sufficient distance from the object to satisfy the separation conditions for a holographic reconstruction [19]. Each reference slit has a scattering area of about $\sim$0.3 μm^2 which is about 1/3 that of the object.

For the experiment, the sample was illuminated with the 25th harmonic ($\lambda = 32$ nm) of the table-top infrared femtosecond laser LUCA (Laser Ultra Court Accordable) at the CEA-Saclay research center, France. The source delivers up to 4×10^{10} photons (0.25 μJ) per pulse, within a spectral bandwidth $\lambda/\Delta\lambda = 150$ and $\sim$20 fs pulse duration [5]. The soft x-ray beam transport and focalization has been optimized using an x-ray wave front sensor [22]. Typically, 2×10^9 photons hit the sample within a focal spot of 5 μm in diameter, corresponding to an intensity of $\sim 10^{11}$ W/cm^2. The transverse and longitudinal coherence lengths at the sample are $\sim$10 μm and $\sim$5 μm, respectively. These are well within the requirements for holography.

We measured the far-field diffraction pattern of the sample exit wave, the hologram, using an x-ray CCD camera [Fig. 1] placed at a distance $z = 20$ mm from the sample. The full CCD chip contains 2048 $\times$ 2048 square pixels with a size $p = 13.5$ μm. The number of incident

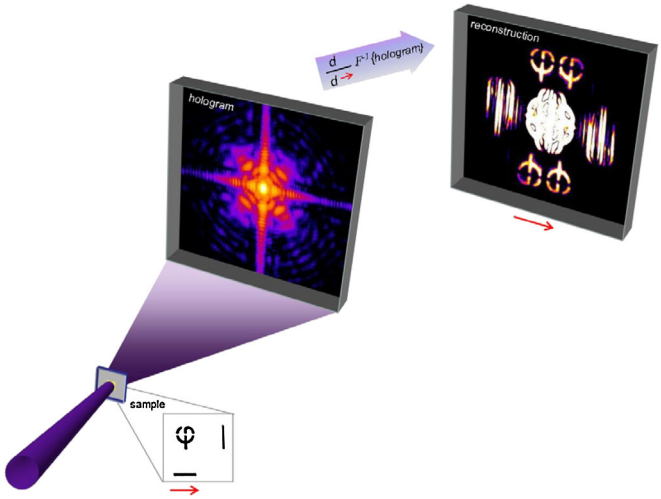

FIG. 1 (color online). Schematic view of the HERALDO experimental setup. Hologram acquisition from sample ("φ" object + reference slits) scattering using a soft x-ray coherent high harmonic beam at 32 nm wavelength. The reconstruction is straightforwardly obtained by computing the directional derivative along the reference slit direction (red arrow) of the inverse Fourier transform of the hologram (i.e., the autocorrelation of the sample transmission). The reconstruction process is symbolized by the operator $\frac{d}{d\rightarrow}F^{-1}\{\text{hologram}\}$.

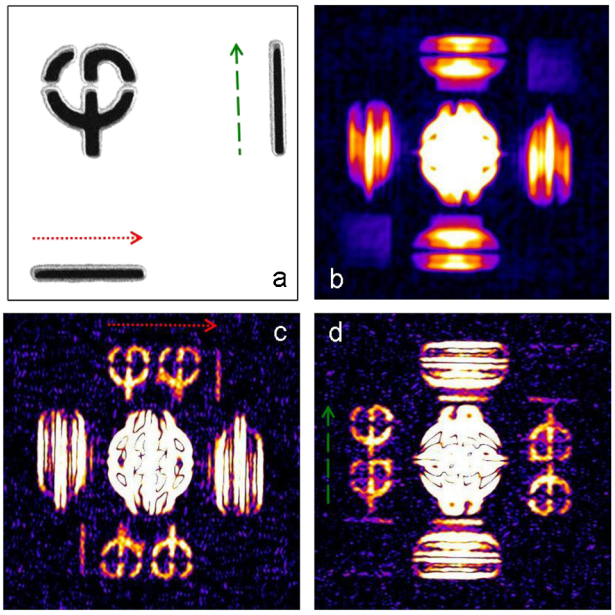

FIG. 2 (color online). Image reconstruction. (a) Scanning electron micrograph (SEM) of the sample showing the "φ" test object and the two references slits (2.1 μm slit length). (b) Field autocorrelation given by the inverse Fourier transform of the hologram. The four cross-correlations of the "φ" object with the references surrounds the central part, as well as the cross-correlation of the two references slits. (c),(d) Numerical derivatives of the field autocorrelation along the two slit directions (indicated by red dotted and green dashed arrows) which lead to the reconstruction of the "φ" object. We obtain two independent images from each extremity of the slit references.

photons diffracted by the sample and detected by the CCD (quantum efficiency of 40% at 32 nm) is about $\sim 2 \times 10^7$ in single shot.

A typical measured hologram is shown in Fig. 3(d). We clearly see the scattering from the two reference slits in the vertical and horizontal axes of the hologram which shows coherent interference with the field scattered from the object. The field autocorrelation [see Fig. 2(b)] is computed from the single-shot hologram through an inverse Fourier transform. The image reconstructions shown in Figs. 2(c) and 2(d) are obtained by computing the derivatives of the field autocorrelation. The design with 2 slits, respectively, horizontal and vertical, provides 4 independent reconstructions, one for each slit extremity, and 4 twin images. Notice that, next to the reconstructed object, each slit end reconstructs also the other reference slit.

From Figs. 2(c) and 2(d) and the field autocorrelation, we get insight into the x-ray intensity distribution on the sample. In particular, the 4 independent reconstructions of the object and the reference exhibit different contrasts, higher for derivation along the horizontal than the vertical slit. Moreover, the references are better illuminated on their inner part (e.g., right side of horizontal slit).

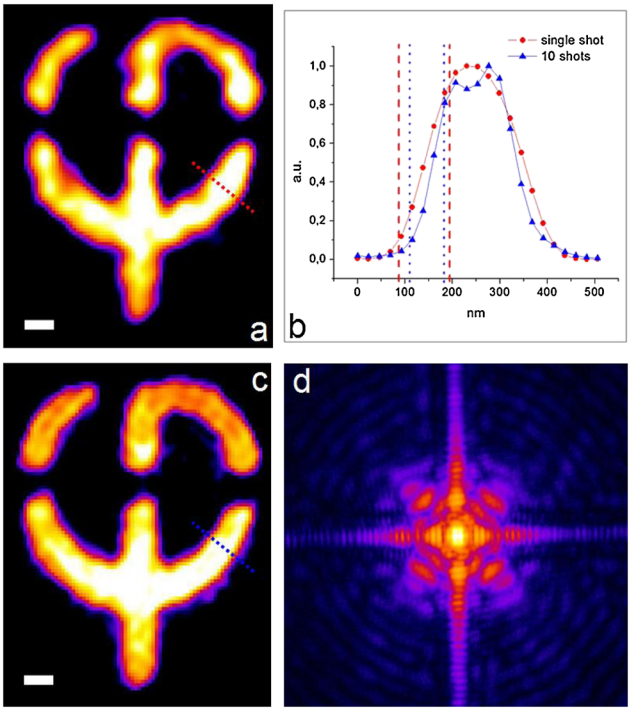

FIG. 3 (color online). Modulus of the final reconstructed image obtained by averaging the 4 independent reconstructions of (a) single shot and (c) 10 shots acquisition. The scale bar is 200 nm and pixel size is 23 nm. (b) Plot profile of the single shot (red line) and 10 shots (blue line) results showing, respectively, a resolution of 105 and 74 nm. (d) Measured hologram of the 10 shots acquisition displayed in logarithmic scale on a 720×720 pixels square which corresponds to 7.63 μm^{-1} maximum spatial frequency.

This inhomogeneous contrast is attributed to the slightly different patterns (slightly different widths) of the two slits, and a decreasing x-ray intensity from the center to the sample periphery. The object however is uniformly illuminated.

In the reconstruction process the hologram was first filtered to select the spatial frequencies with sufficient SNR. A polynomial product was then applied in the Fourier domain [19,20]. This operation, equivalent to a directional derivative in the object space, facilitates differentiation at arbitrary angles. The image quality was improved by subpixel registration [23] and by averaging of the 4 individual complex-valued reconstructions to increase the SNR [17]. Care was also taken to match a global phase between the reconstructions to maximize the signal constructive interference. The final high quality reconstructed image is shown in Fig. 3(a). Using a 10% to 90% edge transition criterion on different edges of the object [see Fig. 3(b) for a typical plot profile], we determined a spatial resolution of 110 nm ($\sim 3.4\lambda$) for the single-shot image. This is in good agreement with the SNR limitation of our measurement at the high scattering angles. The equivalent half period resolution of 110 nm corresponds to a maximum spatial frequency of 4.55 μm^{-1} in the hologram (i.e. a half scattering angle of 144 mrad) above which the scattered signal cannot be extracted due to the noise.

We have performed multishot reconstruction [Fig. 3(c)] by accumulation of 10 shots of 20 fs duration each (the x-ray CCD camera exposure was set to half a second) [see recorded data on Fig. 3(d)]. This was possible because the single-shot exposure is below the damage threshold of the sample. We have estimated, with the multishot reconstruction, the resolution limit given by the manufacturing of the feature size of the reference structures. Using the same resolution criteria as the single-shot we obtained a resolution of 80 nm for the multishot reconstruction [Fig. 3(c)]. Note that the holographic fringes are well resolved and that the scattered signal is observed at a spatial frequency up to 7.63 μm^{-1}. This is above the spatial frequency of 6.25 μm^{-1} (equivalent to 80 nm resolution in the object plane). Practically, the manufacture resolution limit can be estimated by calculating the point spread function (PSF) of the reconstruction using the derivative of the scanning electron micrograph (SEM) image of the slit. This gives us an equivalent resolution limit of 80 nm that is the limit imposed by our HERALDO reference design. We conclude that the resolution for 10 shots acquisition is limited by the slit width designed for the single-shot experiment. But this setup is versatile so that, beyond this experimental demonstration, the width of the reference slit can be easily adjusted to various experimental requirements.

This work enables an efficient future use of holography to capture snapshots of ultrafast phenomena at a nanometer scale using harder x rays. This technique goes beyond the

limitation imposed by conventional Fourier transform holography, in particular, because of the high signal contribution of the reference and effective noise filtering (especially for Poisson limited data) from the reconstruction procedure. The potential for this technique for higher resolution lies in its ability to be scaled down to shorter wavelength. Higher resolution can be obtained by using crystal edges, carbon nanotubes, or metallic nanowires as references to image viruses, cells or nanostructures. For these configurations having a method that is robust against reference defects and nonuniform illumination will be crucial. Our results show that HERALDO has the required robustness and gives good quality reconstructions under significantly inhomogeneous reference illumination and defects. Moreover, the combination of HERALDO with the design of a very large scattering reference [19] could be appropriately used to image weak scatterers such as biomolecules [24,25]. The single-shot demonstration of HERALDO using a soft x-ray femtosecond source also opens other possibilities. First, our femtosecond x-ray flash can take a snapshot of the object before radiation damage occurs. Second, dynamical imaging of nonreproducible ultrafast phenomena at the nanoscale can be performed. The noniterative and unambiguous image reconstruction process makes HERALDO robust to capture space and time amplitude and phase variations associated to complex physical or biological processes. Investigation of ultrafast phase transitions in mesoscopic systems, ultrafast spin reversals of magnetic nanodomains, or large molecule rearrangements in biological environments are some examples of accessible dynamics. Shorter HHG wavelength down to the water window and magnetic L edges can be used for such applications [26–28].

We acknowledge financial support from the EU-LASERLAB (RII3-CT-2003-506350) programs, from French ministry of research though the 2009 ANR grants ''I-NanoX'' and ''Femto-X-Mag'', from the ''Triangle de la Physique'' through the COX grant and the C'NANO research program though the X-NANO grant and also support from the U.S. Department of Energy through the Stanford PULSE Center. We acknowledge Marc Billon, Cédric Baumier, Mike Bogan, Phil Bucksbaum, Franck Fortuna, Julien Gautier, D. Garzella, O. Gobert, J.-F. Hergott, Xiaochi Liu, Jan Lüning, Stefano Marchesini, Alessandra Ravasio, and Philippe Zeitoun for grateful discussion and support.

*hamed.merdji@cea.fr

[1] H. Chapman *et al.*, Nature Phys. **2**, 839 (2006).
[2] H. Chapman *et al.*, Nature (London) **448**, 676 (2007).
[3] A. P. Mancuso *et al.*, New J. Phys. **12**, 035003 (2010).
[4] A. Barty *et al.*, Nat. Photon. **2**, 415 (2008).
[5] A. Ravasio *et al.*, Phys. Rev. Lett. **103**, 028104 (2009).
[6] R. L. Sandberg *et al.*, Opt. Lett. **34**, 1618 (2009).
[7] J. Schwenke *et al.*, J. Mod. Opt. **55**, 2723 (2008).
[8] J. Miao, P. Charalambous, J. Kirz, and D. Sayre, Nature (London) **400**, 342 (1999).
[9] B. Abbey *et al.*, Nature Phys. **4**, 394 (2008).
[10] I. McNulty *et al.*, Science **256**, 1009 (1992).
[11] S. Eisebitt *et al.*, Nature (London) **432**, 885 (2004).
[12] A. S. Morlens *et al.*, Opt. Lett. **31**, 3095 (2006).
[13] G. W. Stroke, *Introduction to Coherent Optics and Holography* (Academic Press, New York, 1969).
[14] J. R. Fienup, Appl. Opt. **21**, 2758 (1982).
[15] A. Szoke, J. Imaging Sci. Technol. **41**, 332 (1997).
[16] H. He *et al.*, Appl. Phys. Lett. **85**, 2454 (2004).
[17] W. F. Schlotter *et al.*, Appl. Phys. Lett. **89**, 163112 (2006).
[18] S. Marchesini *et al.*, Nat. Photon. **2**, 560 (2008).
[19] M. Guizar Sicairos and J. R. Fienup, Opt. Express **15**, 17592 (2007).
[20] M. Guizar Sicairos and J. R. Fienup, Opt. Lett. **33**, 2668 (2008).
[21] S. G. Podorov, K. M. Pavlov, and D. M. Paganin, Opt. Express **15**, 9954 (2007).
[22] J. Gautier *et al.*, Eur. Phys. J. D **48**, 459 (2008).
[23] M. Guizar-Sicairos *et al.*, Opt. Lett. **33**, 156 (2008).
[24] S. Boutet *et al.*, J. Electron Spectrosc. Relat. Phenom. **166–167**, 65 (2008).
[25] T. Shintake, Phys. Rev. E **78**, 041906 (2008).
[26] J. Seres *et al.*, Nature (London) **433**, 596 (2005).
[27] J. Seres *et al.*, Nature Phys. **6**, 455 (2010).
[28] P. Arpin *et al.*, Phys. Rev. Lett. **103**, 143901 (2009).